

The cohesion establishment factor Esco1 acetylates α -tubulin to ensure proper spindle assembly in oocyte meiosis

Yajuan Lu¹, Sen Li², Zhaokang Cui¹, Xiaoxin Dai¹, Mianqun Zhang¹, Yilong Miao¹, Changyin Zhou¹, Xianghong Ou² and Bo Xiong^{1,*}

¹College of Animal Science and Technology, Nanjing Agricultural University, Nanjing 210095, China and ²Fertility Preservation Laboratory, Guangdong Second Provincial General Hospital, Guangzhou 510317, China

Received September 01, 2017; Revised December 19, 2017; Editorial Decision December 22, 2017; Accepted January 02, 2018

ABSTRACT

Esco1 has been reported to function as a cohesion establishment factor that mediates chromosome cohesion and segregation in mitotic cells. However, its exact roles in meiosis have not been clearly defined. Here, we document that Esco1 is expressed and localized to both the nucleus and cytoplasm during mouse oocyte meiotic maturation. Depletion of Esco1 by siRNA microinjection causes the meiotic progression arrest with a severe spindle abnormality and chromosome misalignment, which is coupled with a higher incidence of the erroneous kinetochore–microtubule attachments and activation of spindle assembly checkpoint. In addition, depletion of Esco1 leads to the impaired microtubule stability shown by the weakened resistance ability to the microtubule depolymerizing drug nocodazole and the decreased level of acetylated α -tubulin. Conversely, overexpression of Esco1 causes hyperacetylation of α -tubulin and spindle defects. Moreover, we find that Esco1 binds to α -tubulin and is required for its acetylation. The reduced acetylation level of α -tubulin in Esco1-depleted oocytes can be restored by the ectopic expression of exogenous wild-type Esco1 but not enzymatically dead Esco1-G768D. Purified wild-type Esco1 instead of mutant Esco1-G768D acetylates the synthesized peptide of α -tubulin *in vitro*. Collectively, our data assign a novel function to Esco1 as a microtubule regulator during oocyte meiotic maturation beyond its conventional role in chromosome cohesion.

INTRODUCTION

Meiosis is a specific cell division cycle, which includes a single round of DNA replication, followed by two successive

rounds of chromosome segregation (meiosis I and meiosis II). During meiosis I homologous chromosomes segregate while sister chromatids are still attached to each other; after meiosis II sister chromatids finally segregate (1,2). Correct chromosome segregation requires sister chromatid cohesion, which is formed during replication by the cohesin protein complex (3).

The cohesin complex links DNA molecules and plays key roles in the organization, expression, repair and segregation of eukaryotic genomes. Cohesin is loaded onto chromosomes prior to DNA replication, but loading alone is not sufficient for cohesin-dependent tethering of replicated chromosomes (4–8). The loaded cohesin requires an additional ‘establishment’ step that involves the acetylation of a pair of lysine residues within Smc3 by the evolutionarily conserved cohesin acetyltransferases (9–14). In budding yeast, Eco1 is the acetyltransferase that establishes sister chromatid cohesion during DNA replication (15–18). In addition, Eco1 mutation that genocopies Roberts syndrome has impaired DNA damage repair, reduced ribosomal DNA (rDNA) transcription and aberrant gene expression pattern (17,19). In vertebrates, both Esco1 and Esco2 are establishment determinants which modify cohesin’s Smc3 subunit to establish sister chromatid cohesion during S phase, but differ in their N-terminal domains and expression during development and across the cell cycle (19–25). Also, Esco1 and Esco2 differ dramatically in their interaction with chromatin, as Esco1 is recruited by cohesin to over 11,000 sites, whereas Esco2 is infrequently enriched at REST/NRSF target genes (26). A recent report proposed that cohesion establishment is critically dependent upon Esco2, while Esco1-dependent modification of Smc3 modulates the non-cohesive activities of cohesin, such as DNA repair, transcriptional control and chromosome loop formation (27).

There is increasing evidence suggesting that Esco1 is also involved in tumorigenesis. Esco1 might play an important role in human cancers, and serve as a novel target and prog-

*To whom correspondence should be addressed. Tel: +86 25 8439 9605; Email: xiongbo@njau.edu.cn

nosis factor for human bladder cancer (28). This is a prediction that Esco1 probably participates in many other biological events other than chromosome cohesion. Therefore, more functions and substrates of Esco1 need to be explored. Especially, the roles of Esco1 in meiosis have not been fully defined.

In this report, we find that Esco1 is required for α -tubulin acetylation and microtubule stability, which thereby ensures normal spindle assembly and proper chromosome alignment to orchestrate the mouse oocyte meiotic progression. Our findings also suggest that Esco1 has a novel function beyond chromosome cohesion during oocyte meiosis.

MATERIALS AND METHODS

Antibodies

Rabbit polyclonal anti-Esco1 antibody was purchased from Santa Cruz Biotechnology (Dallas, TX, USA; Cat#:sc-135051); Rabbit polyclonal anti-Esco2 antibody was purchased from Bethyl Laboratories (Montgomery, TX, USA; Cat#: A301-689A-T); mouse monoclonal anti- α -tubulin-fluorescein isothiocyanate (FITC) antibody and mouse monoclonal anti-acetyl- α -tubulin (Lys 40) antibody were purchased from Sigma (St Louis, MO, USA; Cat#: F2168, T7451); human anti-centromere antibody was purchased from Antibodies Incorporated (Davis, CA, USA; Cat#: 15-234); Rabbit polyclonal anti-histone H3 antibody was purchased from Abcam (Cambridge, MA, USA; Cat#: ab1791); Rabbit monoclonal anti-Gapdh antibody was purchased from Cell Signaling Technology (Danvers, MA, USA; Cat#: 2118); HRP-conjugated Streptavidin antibody was purchased from Jackson ImmunoResearch Laboratories (West Grove, PA, USA; Cat#: 016-030-084); FITC-conjugated goat anti-rabbit IgG (H + L), TRITC-conjugated goat anti-rabbit IgG (H + L) and FITC-conjugated goat anti-mouse IgG (H + L) were purchased from Zhongshan Golden Bridge Biotechnology Co., LTD (Beijing, China).

Oocyte collection and culture

All experiments were approved by the Animal Care and Use Committee of Nanjing Agricultural University, China and were performed in accordance with institutional guidelines. Female ICR mice (4–6 weeks) were sacrificed by cervical dislocation after intraperitoneal injections of 5 IU pregnant mare serum gonadotropin for 46 h. Fully-grown oocytes arrested at prophase of meiosis I were collected from ovaries in M2 medium (Sigma, St Louis, MO, USA). Only those immature oocytes displaying a germinal vesicle (GV) were cultured further in M16 medium (Sigma, St Louis, MO, USA) under liquid paraffin oil at 37°C in an atmosphere of 5% CO₂ incubator for *in vitro* maturation. At different time points after culture, oocytes were collected for subsequent analysis.

SiRNA interference

Fully grown GV-intact oocytes were microinjected with 5–10 pl of non-targeting or Esco1-targeting siRNA

(Genepharma, Shanghai, China) in M2 medium containing 2.5 μ M milrinone. The working concentration of siRNA was 25 μ M. To facilitate the degradation of mRNA by siRNA, microinjected oocytes were arrested at GV stage in M16 medium containing 2.5 μ M milrinone for 24 h, and then transferred to milrinone-free M16 medium to resume the meiosis for further experiments. Esco1 siRNA sequences: 5'-GCAUCAUGUUCAG CUGAUATTUAUCAGCUGAACAUUGAUGCTT-3'.

cRNA construct and *in vitro* transcription

Wild-type Esco1 cDNA was sub-cloned into pcDNA3.1/RFP, pcDNA3.1/Flag or pcDNA3.1 vector, respectively. Esco1-G768D, α -tubulin, TubK40Q or TubK40R cDNAs were sub-cloned into pcDNA3.1 vector, respectively. Capped cRNA was synthesized from linearized plasmid using T7 mMessage mMachine kit (ThermoFisher), and purified with MEGAclear kit (ThermoFisher). Typically, 10–12 pl of 0.5–1.0 μ g/ μ l cRNA was injected into oocytes and then arrested at the GV stage in M16 medium containing 2.5 μ M milrinone for 6 h, allowing enough time for translation, followed by releasing into milrinone-free M16 medium for further study. For the overexpression, more than 2.5 μ g/ μ l cRNA was injected into oocytes.

Immunofluorescence and confocal microscopy

Oocytes were fixed in 4% paraformaldehyde in phosphate-buffered saline (PBS) (pH 7.4) for 30 min and permeabilized in 0.5% Triton-X-100 for 20 min at room temperature. Then, oocytes were blocked with 1% bovine serum albumin-supplemented PBS for 1 h and incubated with anti-Esco1 (1:50), anti-acetyl- α -tubulin (Lys-40) (1:100), anti- α -tubulin-FITC (1:300) or anti-centromere (1:200) antibodies at 4°C overnight. After washing four times (5 min each) in PBS containing 1% Tween 20 and 0.01% Triton-X 100, oocytes were incubated with an appropriate secondary antibody for 1 h at room temperature. After washing three times, oocytes were counterstained with Hoechst 33342 (10 μ g/ml) for 10 min. Finally, oocytes were mounted on glass slides and observed under a confocal laser scanning microscope (Carl Zeiss 700).

For measurement of immunofluorescent intensity, the signals from both control and experimental oocytes were acquired by performing the same immunostaining procedure and setting up the same parameters of confocal microscope. Data were analyzed by Image J software.

Immunoprecipitation and immunoblotting analysis

Immunoprecipitation was carried out using 800 oocytes according to the Instructions for ProFound Mammalian Co-Immunoprecipitation Kit (ThermoFisher).

For immunoblotting, a pool of 120 oocytes was lysed in 4 \times Lithium Dodecyl Sulfate (LDS) sample buffer (ThermoFisher, Waltham, MA, USA) containing protease inhibitor, and then separated on 10% Bis-Tris precast gels and transferred onto Polyvinylidene difluoride (PVDF) membranes. The blots were blocked in TBST (Tris-buffered saline

containing 0.1% Tween 20) containing 5% low fat dry milk for 1 h at room temperature and then incubated with anti-Esco1 antibody (1:1000), anti-acetyl- α -tubulin antibody (1:1000) or anti-Flag antibody (1:500) overnight at 4°C. After three times of washes in TBST, the blots were incubated with 1:10 000 dilution of HRP (Horse Radish Peroxidase) conjugated secondary antibodies for 1 h at room temperature. Chemiluminescence was detected with ECL Plus Western Blotting Detection System (GE, Piscataway, NJ, USA) and protein bands were visualized by Tanon-3900. The blots were then stripped and reblotted with anti-Gapdh antibody (1:5000) for loading control.

Purification of Flag-tagged proteins

Full-length Esco1 and mutant Esco1-G768D cDNAs were sub-cloned into pcDNA3.1/Flag vector, respectively, and then transfected into HEK293 cells for protein expression. Cells were lysed in lysis buffer (50 mM Tris-HCl pH8.0, 150 mM NaCl, 1% Triton X-100, 0.1% sodium deoxycholate) and clarified lysates were incubated with anti-Flag M2 agarose beads (Sigma, St Louis, MO, USA; Cat#: F2426). Then, beads were washed 4 \times in wash buffer (PBS, 0.005% NP-40), followed by elution with PBS containing 200 μ g/ml Flag peptide (Sigma, St Louis, MO, USA; Cat#: F4799) and an aliquot of the eluate was analyzed by coomassie staining and western blotting.

In vitro acetylation assay

The Peptide of α -tubulin (Biotin-³¹QPDGQMPSDKTIGG GDDSFN⁵⁰) was synthesized by Qiangyao Biotech (Shanghai, China). For *in vitro* acetylation assay, 1 μ g of α -tubulin peptide was incubated with 250 ng of purified Esco1-Flag or Esco1-G768D-Flag in 50 μ l of acetyltransferase assay buffer (50 mM Tris-HCl pH8.0, 10% glycerol, 10 mM butyric acid, 0.1 mM ethylenediaminetetraacetic acid, 1 mM Dithiothreitol (DTT) and 1 mM Phenylmethanesulfonyl fluoride (PMSF)) with or without 10 μ M Ac-CoA (Sigma) at 30°C for 1 h on a rotating platform. The reaction was then stopped by adding sodium dodecyl sulphate-polyacrylamide gel electrophoresis loading buffer and analyzed by western blotting with anti-acetyl- α -tubulin (Lys 40) antibody.

Statistical analysis

All percentages from at least three repeated experiments were expressed as mean \pm SEM, and the number of oocytes observed was labeled in parentheses (n). Data were analyzed by paired-samples *t*-test, which was provided by GraphPad Prism5 statistical software. The level of significance was accepted as $P < 0.05$.

RESULTS

Esco1 localizes to both chromosomes and cytoplasm during mouse oocyte meiotic maturation

To investigate the role of Esco1 during mouse oocyte meiotic maturation, we first examined its protein expression and subcellular localization pattern. The protein levels of

Esco1 corresponding to different developmental stages during meiotic maturation were examined by western blotting, showing that the amount of Esco1 was increasingly reduced with the meiotic progression (Figure 1A and Supplementary Figure S1). Microinjection of Esco1-RFP cRNA revealed that Esco1-RFP was predominantly localized to the chromosomes, but also distributed in the cytoplasm, especially on the spindle apparatus (Figure 1B). This spindle-localization pattern was confirmed by the immunofluorescence analysis of endogenous Esco1 by antibody staining (Supplementary Figure S2). To further verify the distribution of Esco1, we isolated the germinal vesicles from GV oocytes and then tested the presence of Esco1 in the nucleus and cytoplasm by western blotting (Figure 1C). As shown in Figure 1D, the blots were probed with anti-H3 antibody as an indicator of nucleus fraction and probed with anti-Gapdh antibody as an indicator of cytoplasm fraction. From the blot probed with anti-Esco1 antibody, we observed that the robust bands of Esco1 were present in the GV as well as the cytoplasm without the GV corresponding to the intact oocytes (Figure 1D), demonstrating that a pool of Esco1 indeed localizes in the cytoplasm during oocyte meiosis.

Depletion of Esco1 impairs the normal meiotic progression and provokes spindle assembly checkpoint during oocyte meiosis

To clearly define the function of Esco1, loss-of-function experiments via gene-targeting siRNA microinjection were performed to silence Esco1 in the oocytes. After injection, oocytes were arrested at the GV stage in medium with milrinone for 24 h to fully degrade Esco1 mRNA. A significant reduction of Esco1 protein level was observed in Esco1-depleted oocytes compared to controls by both immunofluorescence and western blotting analysis (Figure 2A and Supplementary Figure S3), revealing that Esco1 was successfully depleted by RNAi. Also, depletion of Esco1 did not affect the localization and protein level of Esco2 (Supplementary Figure S4). During oocyte meiotic maturation, oocytes experience a series of consecutive events including germinal vesicle breakdown (GVBD), spindle assembly and chromosome alignment at the metaphase plate, homologous chromosome segregation, first polar body extrusion (PBE), and then arrest at metaphase II stage waiting for fertilization. To figure out if depletion of Esco1 has effects on the meiotic resumption, the rates of GVBD and PBE were examined after knockdown. The statistical result revealed that GVBD was not affected after Esco1 depletion ($83.4 \pm 2.3\%$, $n = 134$ versus $85.2 \pm 2.1\%$, $n = 145$ control; Supplementary Figure S5), but the ratio of PBE was remarkably lower in Esco1-depleted oocytes than that in control oocytes ($43.8 \pm 4.6\%$, $n = 222$ versus $75.3 \pm 3.0\%$, $n = 171$ control, $P < 0.01$; Figure 2B and C), indicating Esco1 is required for mouse oocyte meiotic progression. To rule out the possibility that the meiotic failure we observed was caused by the off-target effect of siRNA, we expressed the exogenous Esco1 in Esco1-depleted oocytes and found that PBE rate was increased to the level indistinguishable from the controls ($65.4 \pm 2.8\%$, $n = 173$, $P < 0.05$; Figure 2B and C).

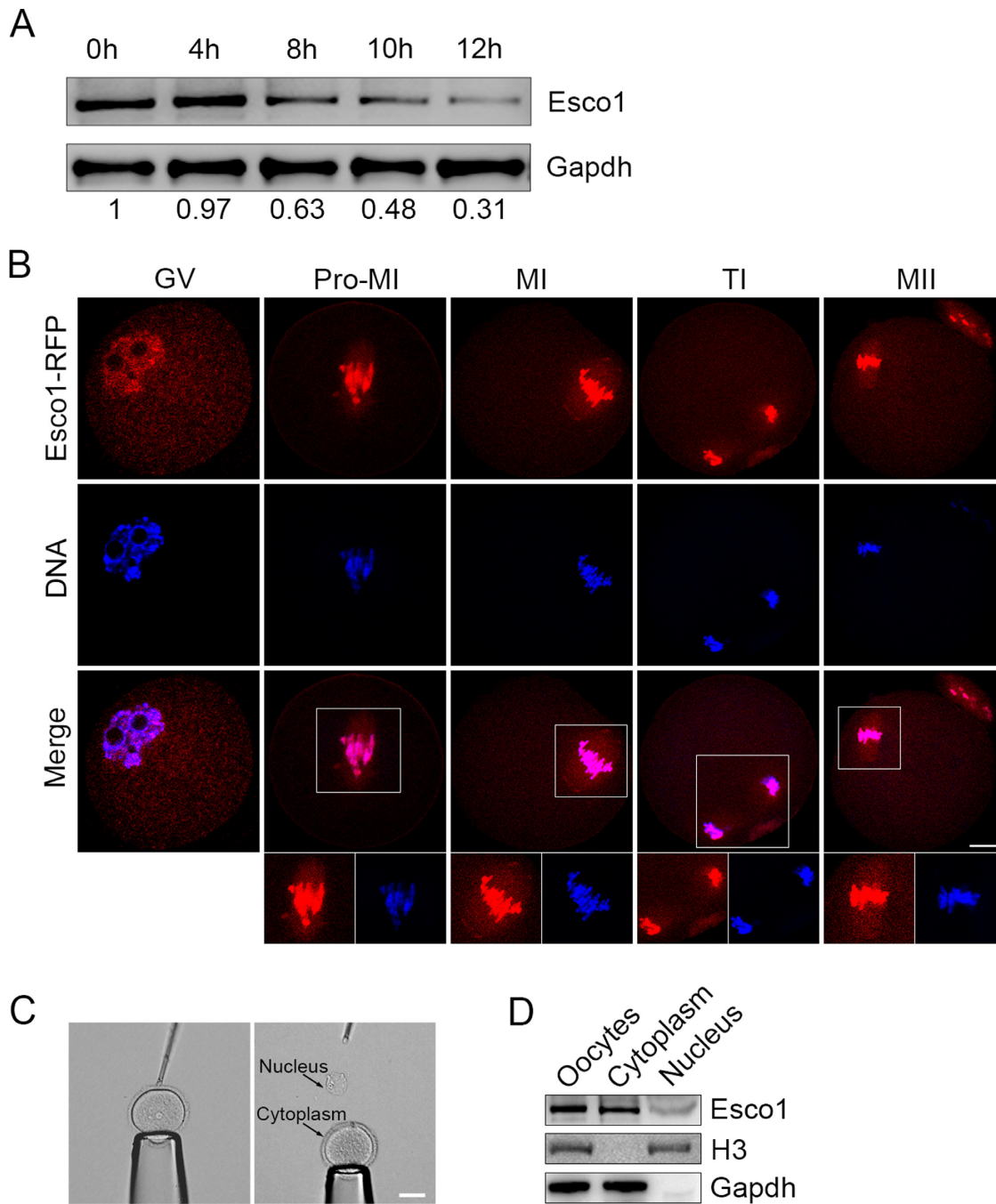


Figure 1. Protein expression and subcellular localization of Esco1 during mouse meiotic maturation. **(A)** Protein levels of Esco1 at specific time point corresponding to various developmental stages during meiotic maturation: 0 h, GV; 4 h, Pro-M I (prometaphase I); 8 h, M I (metaphase I); 10 h, T I (telophase I); 12 h, M II (metaphase II). The blots were probed with anti-Esco1 antibody and anti-Gapdh antibody, respectively. **(B)** Mouse oocytes at GV, Pro-M I, M I, T I and M II stages were microinjected with Esco1-RFP cRNA (red) and counterstained with Hoechst (blue). Images were acquired under the confocal microscope. Scale bar, 20 μ m. The relative fluorescent intensity of Esco1 signals in the nucleus/cytoplasm in GV oocytes was 0.35. **(C)** Representative image of the oocyte before and after isolation of GV. Scale bar, 40 μ m. **(D)** Protein levels of Esco1 in intact oocytes, cytoplasm and GV (nucleus). The blots were probed with anti-Esco1 antibody, anti-H3 antibody and anti-Gapdh antibody, respectively. The relative gray value of Esco1 bands in the nucleus/cytoplasm was 0.32.

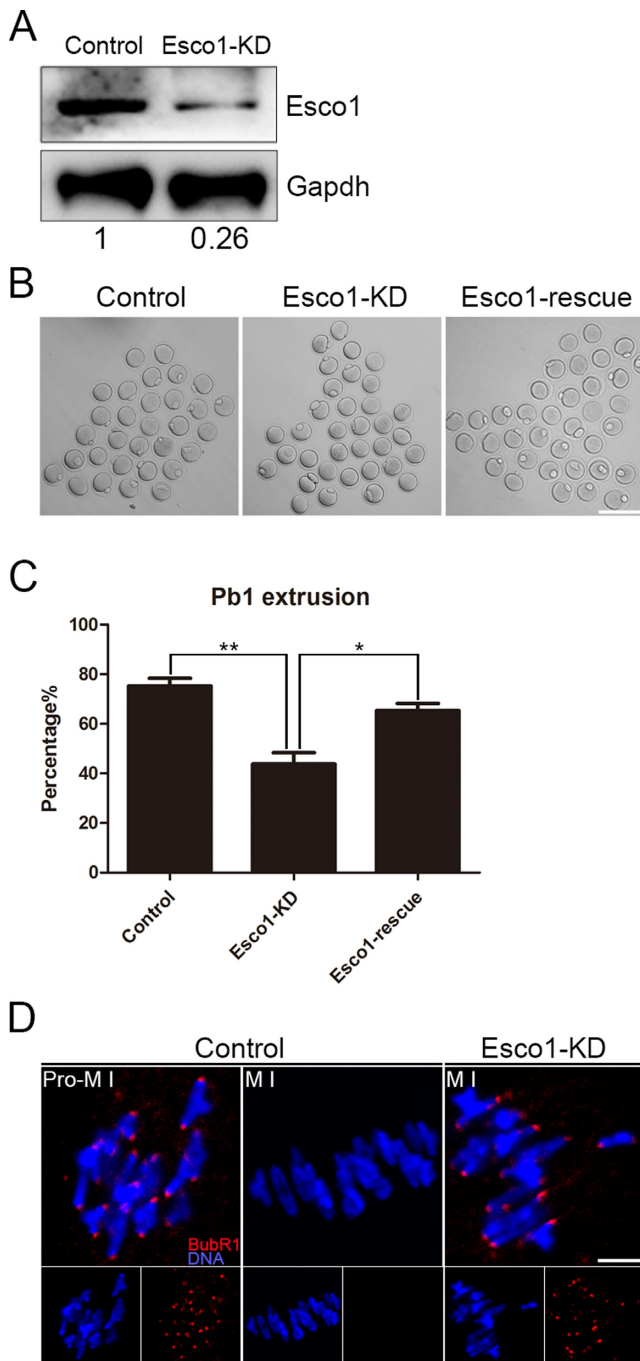


Figure 2. Depletion of Esco1 causes meiotic arrest and activation of SAC in M I oocytes. (A) Protein levels of Esco1 in control and Esco1-KD (siRNA microinjected) oocytes. The blots were probed with anti-Esco1 antibody and anti-Gapdh antibody, respectively. (B) Representative images of PBE in control, Esco1-KD and Esco1-rescue oocytes. Scale bar, 200 μ m. (C) Quantitative analysis of PBE rate in control, Esco1-KD and Esco1-rescue oocytes. Data were presented as mean percentage (mean \pm SEM) of at least three independent experiments. * $P < 0.05$, ** $P < 0.01$. (D) The localization of BubR1 in control and Esco1-KD oocytes at Pro-M I and M I stages. Oocytes were immunostained with anti-BubR1 antibody and counterstained with Hoechst. Scale bar, 2.5 μ m.

A higher rate of meiotic arrest in the absence of Esco1 suggests that spindle assembly checkpoint (SAC) might be activated. To gain insight into this issue, mouse oocytes from control and Esco1-depleted groups were firstly immunostained with the antibody of BubR1, an integral part of SAC, to indicate the SAC activation. In controls, BubR1 was localized to the unattached kinetochores at pro-metaphase I stage, but lost this localization pattern at metaphase I stage when kinetochores are properly attached (Figure 2D). However, Esco1 depletion remained the kinetochore localization of BubR1 at metaphase I stage, indicative of activation of SAC (Figure 2D).

Esco1 maintains correct spindle assembly, chromosome alignment and kinetochore–microtubule attachments in oocytes

In most cases SAC is activated when spindle assembly and chromosome alignment suffer from the damage. To test this, metaphase I oocytes were immunolabeled with anti- α -tubulin antibody to observe the spindle morphologies and counterstained with Hoechst to visualize the chromosome alignment. As expected, control oocytes at metaphase I stage usually showed a typical barrel-shape spindle with the well-aligned chromosomes at the equator (Figure 3A). By striking contrast, we found a higher percentage of spindle organization defects ($60.8 \pm 2.1\%$, $n = 105$ versus $20.6 \pm 2.4\%$, $n = 99$ control, $P < 0.001$; Figure 3A and B) and chromosome alignment failure ($48.4 \pm 2.8\%$, $n = 105$ versus $19.3 \pm 0.5\%$, $n = 99$ control, $P < 0.001$; Figure 3A and D) in Esco1-depleted oocytes, displaying a majority of short or wide-polar spindles with one or several scattered or lagging chromosomes (short: $30.3 \pm 3.1\%$, $n = 105$ versus $5.1 \pm 1.0\%$, $n = 99$ control, $P < 0.01$; wide-polar: $24.8 \pm 1.3\%$, $n = 105$ versus $9.4 \pm 2.2\%$, $n = 99$ control, $P < 0.01$; elongated: $5.7 \pm 1.5\%$, $n = 105$ versus $6.1 \pm 0.4\%$, $n = 99$ control; Figure 3A and C). The defects of spindle formation were confirmed by timepoint imaging spanning the entire meiosis I (2 h: $16.1 \pm 3.1\%$, $n = 31$ versus 0% , $n = 30$ control; 4 h: $26.8 \pm 2.0\%$, $n = 34$ versus $2.8 \pm 2.8\%$, $n = 34$ control, $P < 0.01$; 6 h: $44.3 \pm 3.0\%$, $n = 35$ versus $8.7 \pm 0.7\%$, $n = 35$ control, $P < 0.001$; 8 h: $53.9 \pm 3.9\%$, $n = 37$ versus $21.1 \pm 2.0\%$, $n = 33$ control, $P < 0.01$; 10 h: $57.4 \pm 1.8\%$, $n = 35$ versus $23.9 \pm 1.7\%$, $n = 38$ control, $P < 0.001$; Supplementary Figure S6A and B) and can be restored by expressing exogenous Esco1 (control: $19.4 \pm 0.6\%$, $n = 32$, $P < 0.001$; Esco1-KD: $56.4 \pm 4.0\%$, $n = 30$; Esco1-rescue: $34.1 \pm 4.2\%$, $n = 30$, $P < 0.05$; Supplementary Figure S7A and B). Furthermore, we measured the width of chromosome plate at M I stage and found it remarkably wider in Esco1-depleted oocytes over the controls ($19.8 \pm 1.2 \mu$ m, $n = 105$ versus $12.7 \pm 1.2 \mu$ m, $n = 99$ control, $P < 0.05$; Figure 3E).

The remarkably higher frequency of misaligned chromosomes implied that the compromised K–MT attachments might occur in Esco1-depleted oocytes. To directly visualize the K–MT interaction, we immunostained kinetochores with CREST and microtubules with anti- α -tubulin antibody following cold treatment which could depolymerize the unstable microtubules that are not attached to kinetochores. By confocal scanning we found that in most of control oocytes kinetochores at the well-aligned chromosome remained fully attached by the microtubule fibers after cold

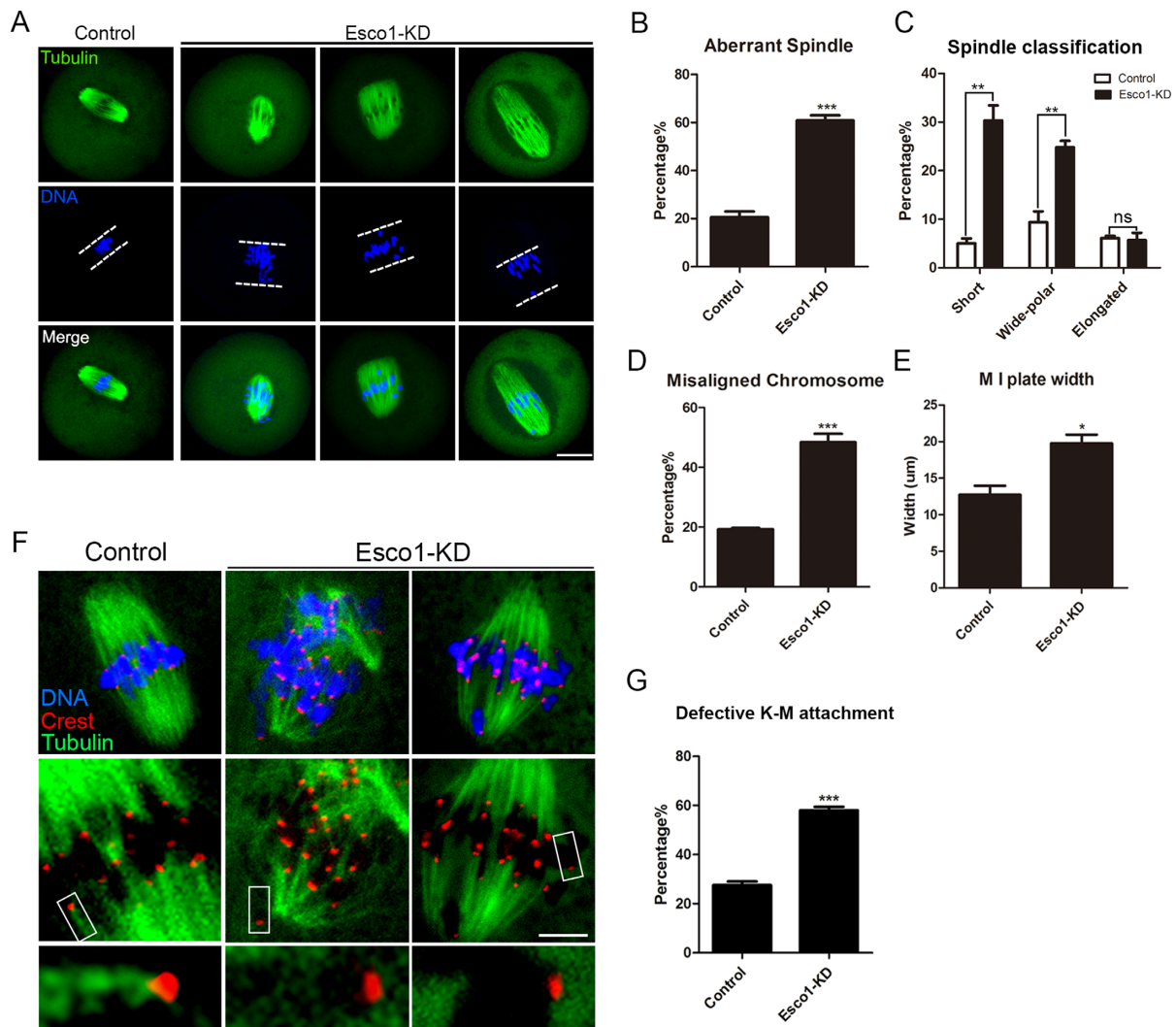


Figure 3. Depletion of Esco1 results in spindle assembly, chromosome alignment and K-M attachment abnormalities during meiotic maturation. (A) Representative images of spindle morphologies and chromosome alignment in control and Esco1-KD oocytes. Oocytes were immunostained with anti- α -tubulin-FITC antibody to visualize spindles and counterstained with Hoechst to visualize chromosomes. Scale bar, 20 μ m. (B) The rate of aberrant spindles was recorded in control and Esco1-KD oocytes. (C) The rates of short, wide polar and elongated spindles were recorded in control and Esco1-KD oocytes. (D) The rate of misaligned chromosomes was recorded in control and Esco1-KD oocytes. (E) The width of M I plate was measured in control and Esco1-KD oocytes. (F) Representative images of kinetochore-microtubule attachments in control and Esco1-KD oocytes. Oocytes were immunostained with anti- α -tubulin-FITC antibody to visualize spindles, with CREST to visualize kinetochores and counterstained with Hoechst to visualize chromosomes. Scale bar, 5 μ m. (G) The rate of defective kinetochore-microtubule attachments was recorded in control and Esco1-KD oocytes. Data of (B), (C), (D), (E) and (G) were presented as mean percentage (mean \pm SEM) of at least three independent experiments. * $P < 0.05$, ** $P < 0.01$, *** $P < 0.001$.

treatment (Figure 3F and G). However, in Esco1-depleted oocytes, a significantly increased proportion of scattered kinetochores with very few cold-stable microtubules were observed by performing quantitative analysis ($57.9 \pm 1.5\%$, $n = 57$ versus $27.6 \pm 1.4\%$, $n = 58$ control, $P < 0.001$; Figure 3F and G). These K-MT attachment errors would inevitably result in the establishment of unstable chromosome biorientation, which is probably associated with the meiotic defects observed in Esco1-depleted oocytes.

Esco1 binds to α -tubulin and is essential for its acetylation to regulate microtubule stability in oocytes

Impaired spindle assembly in the absence of Esco1 prompted us to further examine the involvement of Esco1

in the microtubule stability. To verify this hypothesis, we tested the microtubule resistance to the microtubule depolymerizing drug nocodazole. In control oocytes, 5 min after nocodazole treatment, although spindle morphologies were collapsed, microtubule fibers still persisted (Figure 4A). In striking contrast, following the same treatment, microtubules were completely depolymerized in Esco1-depleted oocytes, showing the weakened microtubule stability in these oocytes (Figure 4A).

We next determined the acetylated level of α -tubulin on Lys 40, a marker of stabilized microtubules, to assess the microtubule stability in oocytes. The immunostaining was carried out using anti-acetylated tubulin antibody which recognizes an epitope located on the α -tubulin within four residues of Lys 40 when this amino acid is acetylated.

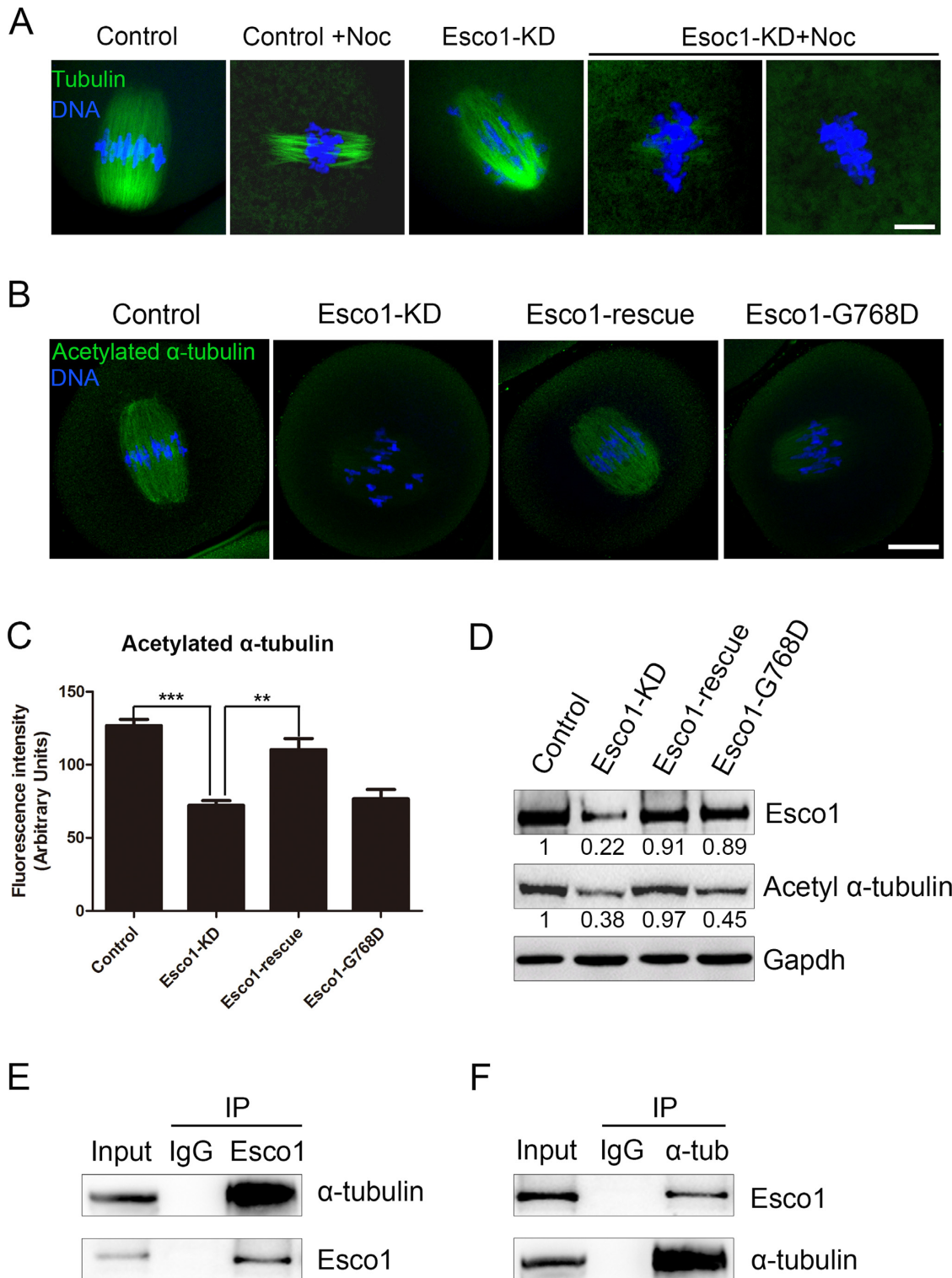


Figure 4. Depletion of Esco1 impairs microtubule stability in mouse oocytes. **(A)** Representative images of microtubules before and after 5 min of treatment with nocodazole in control and Esco1-KD oocytes. Oocytes were immunostained with anti- α -tubulin-FITC antibody to visualize microtubules and counterstained with Hoechst to visualize chromosomes. Scale bar, 5 μ m. **(B)** Representative images of acetylated α -tubulin in control, Esco1-KD, Esco1-rescue and Esco1-G768D oocytes. Oocytes were immunostained with anti-acetylated α -tubulin antibody and counterstained with Hoechst to visualize chromosomes. Scale bar, 20 μ m. **(C)** The immunofluorescence intensity was recorded in control, Esco1-KD, Esco1-rescue and Esco1-G768D oocytes. Data were presented as mean percentage (mean \pm SEM) of at least three independent experiments. $**P < 0.01$, $***P < 0.001$. **(D)** Protein levels of acetylated α -tubulin in control and Esco1-KD oocytes were determined by western blotting. The blots of control and Esco1-KD oocytes were probed with anti-Esco1, anti-acetylated α -tubulin and anti-Gapdh antibodies, respectively. **(E)** Co-IP was performed to determine the interaction between Esco1 and α -tubulin. Oocyte lysates were incubated with IgG and anti-Esco1 antibody, respectively, followed by incubation with protein G beads. The blots of IP eluates were probed with anti- α -tubulin and anti-Esco1 antibodies, respectively. **(F)** Reciprocal Co-IP was performed with IgG and anti- α -tubulin antibody, respectively. The blots of IP eluates were probed with anti-Esco1 and anti- α -tubulin antibodies, respectively.

The result showed that *Esco1*-depleted oocytes displayed a markedly decreased fluorescent intensity of acetylated α -tubulin compared to control oocytes (72.2 ± 3.2 , $n = 39$ versus 126.8 ± 4.3 , $n = 45$ control, $P < 0.001$; Figure 4B and C). Also, the reduced acetylation level of α -tubulin in *Esco1*-depleted oocytes could be restored by ectopic expression of exogenous wild-type *Esco1* rather than enzymatically dead *Esco1*-G768D (110.4 ± 7.6 , $n = 30$ versus 76.7 ± 6.4 , $n = 30$, $P < 0.01$; Figure 4B and C). The measurement of fluorescent intensity of α -tubulin indicated that the changes of acetylated α -tubulin in *Esco1*-depleted and *Esco1*-rescue oocytes were not due to the alteration of total amount of microtubules (control: 91.2 ± 7.6 , $n = 32$; *Esco1*-KD: 87.6 ± 3.5 , $n = 30$; *Esco1*-rescue: 96.6 ± 6.5 , $n = 35$; Supplementary Figure S7A and C). The fluorescence data was further verified by the western blotting analysis (Figure 4D), suggesting that acetyltransferase activity of *Esco1* is essential for α -tubulin acetylation. Moreover, we performed Co-IP to determine the interaction between *Esco1* and α -tubulin. Immunoprecipitation was first performed with *Esco1* antibody. The blot of IP eluate probed by *Esco1* antibody showed that *Esco1* was specifically present in the antibody group instead of IgG control group (Figure 4E), suggesting that the complex containing *Esco1* was pulled down in the eluate. Meanwhile, the blot probed by α -tubulin antibody also showed the exclusive presence of α -tubulin in the antibody group (Figure 4E). Reciprocally, *Esco1* was specifically present in the IP eluate which was pulled down by α -tubulin antibody (Figure 4F), indicating that *Esco1* interacts with α -tubulin in oocytes.

We further expressed the acetylation mutants of α -tubulin in *Esco1*-depleted oocytes to test whether the abnormal spindle assembly is caused by the defective acetylation of α -tubulin on Lys 40. The result showed that expression of whether TubK40Q acetylmimic mutant or TubK40R non-acetylatable mutant into wild-type oocytes would compromise the normal spindle formation, indicating that maintenance of acetylation level of α -tubulin is critical for microtubule stability (control: $17.7 \pm 2.9\%$, $n = 40$; TubK40R: $35.0 \pm 1.7\%$, $n = 37$, $P < 0.01$; TubK40Q: $54.6 \pm 6.1\%$, $n = 39$, $P < 0.01$; Supplementary Figure S8). Notably, TubK40Q but not TubK40R mutation restored the aberrant spindle assembly (control: $20.0 \pm 1.9\%$, $n = 90$, $P < 0.001$; *Esco1*-KD: $57.8 \pm 2.9\%$, $n = 82$; *Esco1*-KD + TubK40R: $51.1 \pm 4.8\%$, $n = 80$; *Esco1*-KD + TubK40Q: $30.0 \pm 5.1\%$, $n = 85$, $P < 0.01$; Figure 5A and B) and misaligned chromosomes in *Esco1*-depleted oocytes (control: $17.7 \pm 2.3\%$, $n = 90$, $P < 0.01$; *Esco1*-KD: $55.5 \pm 6.2\%$, $n = 82$; *Esco1*-KD + TubK40R: $48.9 \pm 2.9\%$, $n = 80$; *Esco1*-KD + TubK40Q: $33.3 \pm 3.9\%$, $n = 85$, $P < 0.05$; Figure 5A and C). However, expression of wild-type α -tubulin in *Esco1*-depleted oocytes could not restore the spindle defects, suggesting that lack of acetylated α -tubulin causes the spindle defects in *Esco1*-depleted oocytes (control: $18.9 \pm 1.1\%$, $n = 36$, $P < 0.001$; *Esco1*-KD: $58.0 \pm 3.0\%$, $n = 37$; Tub: $51.5 \pm 5.4\%$, $n = 34$; Supplementary Figure S9).

Taken together, these observations reveal that *Esco1* plays an important role in spindle assembly via modulating α -tubulin acetylation-mediated microtubule stability.

Overexpression of *Esco1* leads to hyperacetylation of α -tubulin and spindle defects

Because hyperacetylation of α -tubulin induced by depletion of Hdac3 (29) or expression of TubK40Q acetylmimic mutant perturb the spindle organization in oocytes (Supplementary Figure S8), we wanted to test whether *Esco1* overexpression would have similar effects. *Esco1*-Flag cRNA was injected into GV oocytes followed by culturing to M I stage to perform the analysis. The expression of *Esco1*-Flag was detected by the western blotting using Flag antibody, showing the presence of band in the *Esco1*-overexpressed oocytes instead of controls (Figure 6A). Immunostaining and western blotting results revealed that overexpression of *Esco1* caused the considerable increase in the acetylated level of α -tubulin compared to controls (139.8 ± 6.9 , $n = 36$ versus 95.1 ± 4.2 , $n = 34$ control, $P < 0.01$; Figure 6A–C). Moreover, a large number of impaired spindles with elongated or multipolar morphologies and misaligned chromosomes was observed in *Esco1*-overexpressed oocytes (spindle: $67.9 \pm 2.9\%$, $n = 38$ versus $19.4 \pm 1.4\%$, $n = 41$ control, $P < 0.001$; chromosome: $54.6 \pm 4.6\%$, $n = 38$ versus $17.0 \pm 1.7\%$, $n = 41$ control, $P < 0.01$; Figure 6D–F), consequently resulting in the failure of PBE ($47.3 \pm 5.0\%$, $n = 115$ versus $75.8 \pm 2.5\%$, $n = 108$ control, $P < 0.01$; Figure 6G).

Esco1 acetylates α -tubulin on Lys 40 *in vitro*

To ask whether *Esco1* is able to acetylate α -tubulin on Lys 40 *in vitro*, both *Esco1*-Flag and enzymatically dead *Esco1*-G768D-Flag were purified from HEK293 cells by Flag purification. The identity of purified proteins was confirmed by both coomassie staining and western blotting with anti-*Esco1* antibody (Figure 7A). The synthesized peptide which is composed of amino acid sequence from 31 to 50 of α -tubulin with N-terminal biotin was identified by western blotting analysis with streptavidin and mass spectrometry (Figure 7B and Supplementary Figure S10). Then we performed *in vitro* acetylation assay using the purified proteins and synthesized peptide. The result showed that the peptide of α -tubulin was acetylated on Lys 40 in the presence of *Esco1*-Flag and Ac-CoA in an *in vitro* reaction system (Figure 7C). Conversely, *Esco1*-G768D-Flag had no acetyltransferase activity toward the peptide of α -tubulin under the same condition (Figure 7C). Thus, we conclude that *Esco1* could directly acetylate α -tubulin on Lys 40.

DISCUSSION

In budding yeast, there is only one acetyltransferase *Eco1* that acetylates cohesion subunit *Smc3* to establish chromosome cohesion. However, in mammalian cells, it evolves into two acetyltransferases *Esco1* and *Esco2* to exert this function. Although *Esco1* and *Esco2* have redundant roles in chromosome cohesion, they exert different functions in other biological processes through their distinct substrates. Compared to *Esco2*, *Esco1* has not been well studied in both mitosis and meiosis, especially regarding the functions beyond chromosome cohesion.

To investigate the role of *Esco1* in mouse oocytes, we first of all detected its protein expression and subcellular localization during meiotic progression. Unexpectedly, we

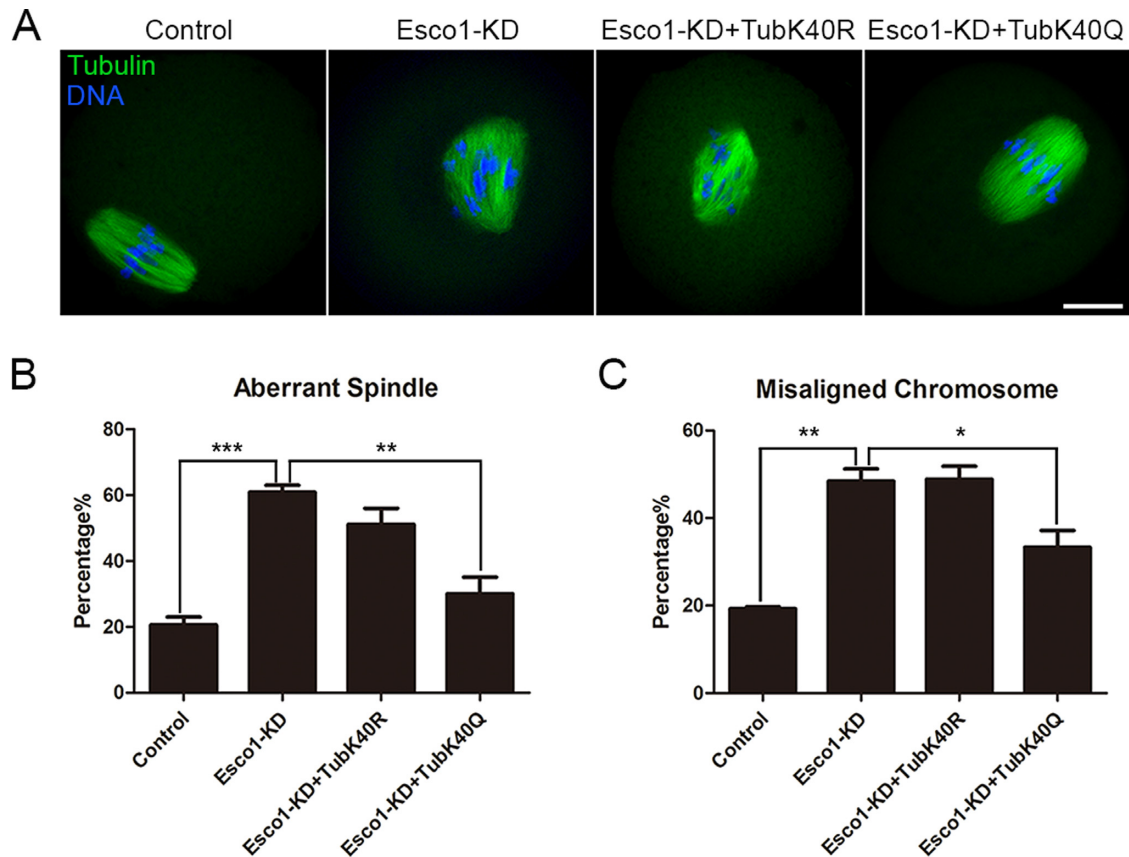


Figure 5. TubK40Q rescues the defective spindle assembly and chromosome alignment in Esco1-depleted oocytes. (A) Representative images of spindle morphologies and chromosome alignment in control, Esco1-KD, Esco1-KD + TubK40R and Esco1-KD + TubK40Q oocytes. Oocytes were immunostained with anti- α -tubulin-FITC antibody to visualize spindles and counterstained with Hoechst to visualize chromosomes. Scale bar, 20 μ m. (B) The rate of defective spindle assembly was recorded in control, Esco1-KD, Esco1-KD + TubK40R and Esco1-KD + TubK40Q oocytes. (C) The rate of misaligned chromosomes was recorded in control, Esco1-KD, Esco1-KD + TubK40R and Esco1-KD + TubK40Q oocytes. Data of (B) and (C) were presented as mean percentage (mean \pm SEM) of at least three independent experiments. * $P < 0.05$, ** $P < 0.01$, *** $P < 0.001$.

not only observed the chromosome localization of Esco1, but also found a large amount of Esco1 in the cytoplasm, with a special accumulation on the spindle apparatus. In yeast, inactivation of Ecol or Eso1 after S phase did not affect sister chromatid cohesion (24,30,31). This result has been generally interpreted as them being cohesion factors involved in establishment. In mammalian females, cohesion is established when meiotic DNA replication and recombination occur in fetal oocytes. After birth, oocytes arrest at the prolonged dictyate stage until recruited to grow into mature oocytes that divide at ovulation, but bivalent cohesion is maintained without detectable turnover (32,33). Coupled with our observation that Esco1 is localized to both chromosomes and spindles, we propose that Esco1 might have a particular function during oocyte meiotic maturation.

To this end, loss-of-function experiments via gene-targeting siRNA microinjection were performed to silence Esco1 in the oocytes. The depletion caused a higher rate of meiotic arrest, suggesting that SAC was activated and spindle structure or chromosome alignment might be disrupted. As expected, immunostaining result showed that SAC component BubR1 persisted in residing on the kinetochores at M I stage in Esco1-depleted oocytes, indicative of activation of SAC. Also various abnormal spindle morphologies

and misaligned chromosomes were observed, accompanied by the defective K–M attachments, which resultantly provoked the SAC.

The spindle defects in the absence of Esco1 prompted us to further examine the involvement of Esco1 in the microtubule stability. Our findings prove that depletion of Esco1 weakens the microtubule resistance to microtubule depolymerizing drug nocodazole. It has been shown that tubulin acetylation increases the stability of microtubules to protect against mechanical breakage (34,35). We thus tested the acetylation level of α -tubulin in Esco1-depleted oocytes. Tubulin acetylation that occurs on Lys-40 of the α -tubulin subunit is found in both somatic cells and mouse oocytes as an indicator of stabilized microtubules (36–39). Silencing of histone deacetylases such as Hdac3 and Hdac6 modulates the acetylation level of α -tubulin to promote spindle assembly and meiotic process in oocytes (29,40). We find that depletion of Esco1 resulted in the pronounced decrease in signals of acetylated α -tubulin by both immunofluorescence and western blotting analyses. Meanwhile, overexpression of Esco1 led to hyperacetylation of α -tubulin and spindle defects, suggesting that the balance of acetylated level of α -tubulin is critical for normal spindle assembly. Notably, our findings demonstrate that Esco1 binds to α -tubulin and is

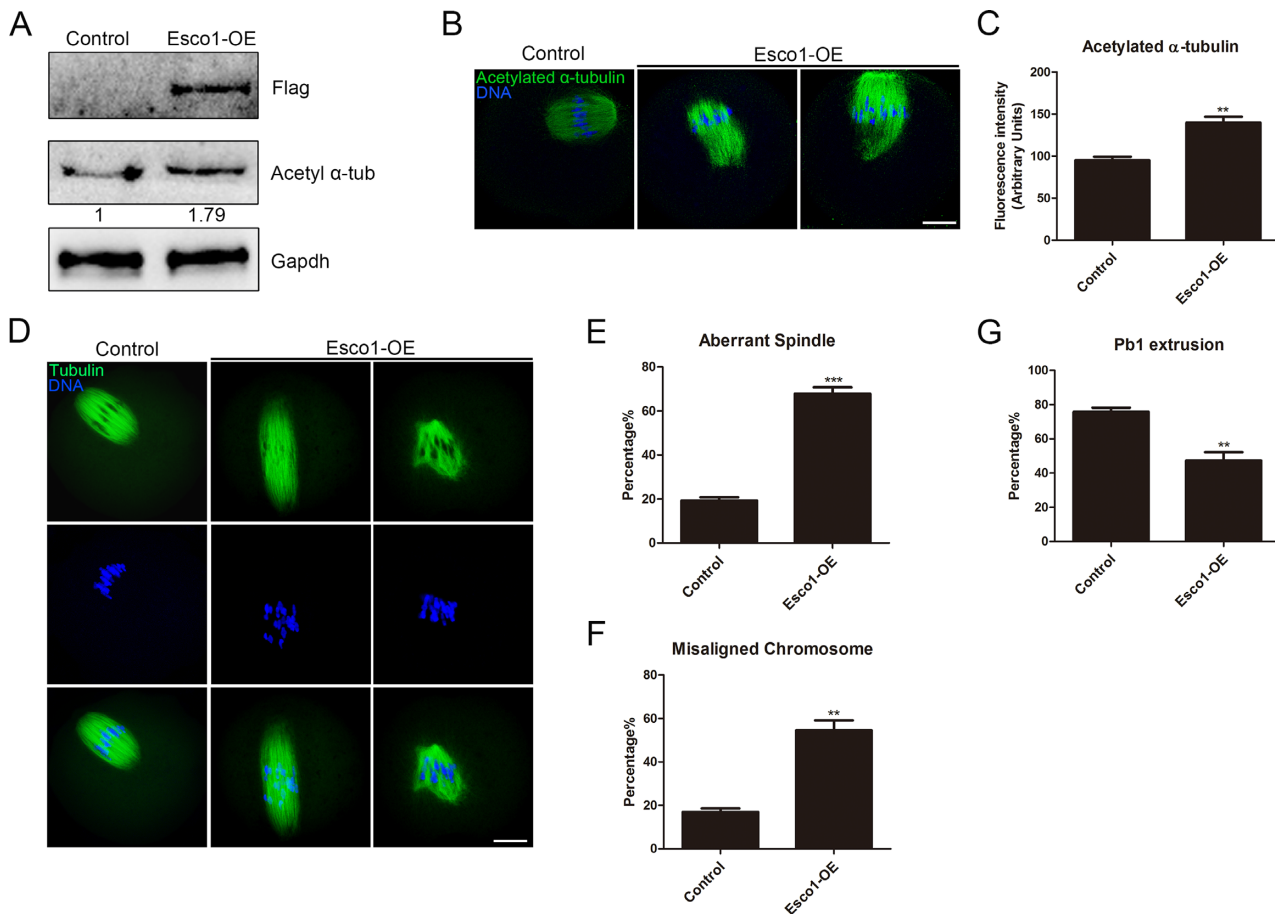


Figure 6. Overexpression of Esco1 increases the acetylation level of α -tubulin and perturb the spindle assembly. (A) Protein levels of Esco1-Flag in control and Esco1-OE (overexpression) oocytes. The blots were probed with anti-Flag antibody, anti-acetyl- α -tubulin antibody and anti-Gapdh antibody, respectively. (B) Representative images of acetylated α -tubulin in control and Esco1-OE oocytes. Oocytes were immunostained with anti-acetyl- α -tubulin antibody and counterstained with Hoechst to visualize chromosomes. Scale bar, 20 μ m. (C) The immunofluorescence intensity was recorded in control and Esco1-OE oocytes. (D) Representative images of spindle morphologies and chromosome alignment in control and Esco1-OE oocytes. Oocytes were immunostained with anti- α -tubulin-FITC antibody to visualize spindles and counterstained with Hoechst to visualize chromosomes. Scale bar, 20 μ m. (E) The rate of aberrant spindles was recorded in control and Esco1-OE oocytes. (F) The rate of misaligned chromosomes was recorded in control and Esco1-OE oocytes. (G) Quantitative analysis of PBE rate in control and Esco1-OE oocytes. Data of (C), (E), (F) and (G) were presented as mean percentage (mean \pm SEM) of at least three independent experiments. ** $P < 0.01$, *** $P < 0.001$.

required for its acetylation. Wild-type but not catalytically dead mutation of Esco1 could rescue the reduced acetylation level of α -tubulin in depletion of Esco1. Furthermore, TubK40Q acetylmimic mutation but not TubK40R non-acetylatable mutation rescued the defective spindle assembly in the Esco1-depleted oocytes. Finally, we carried out the *in vitro* acetylation assay using the purified proteins and synthesized peptide to show that Esco1 directly acetylates α -tubulin on Lys 40. Therefore, these observations reveal that Esco1 plays an important role in the regulation of microtubule stability via maintaining the acetylation of α -tubulin.

It has been recently reported that Esco1 and Esco2 exert distinct and separable activities of cohesin in somatic cells (27). Esco1 is active throughout the cell cycle but has very little effect on mitotic cohesion, while Esco2 modifies cohesin only during S phase and is a dominant determinant of cohesion establishment (27). Thus, two distinct pathways regulate cohesin in vertebrates: Esco2 is required for cohesion between sister chromatids, and Esco1 promotes other

non-cohesive functions of cohesin, such as maintenance of chromosome structure (27). In addition, Esco1 and Esco2 must have other unknown substrates because of their nature of acetyltransferase. We have previously documented that Esco2 modulates SAC and kinetochore functions to ensure the euploidy of eggs via maintaining H4K16 acetylation status during mouse oocyte meiosis (41). In the present study, we identify α -tubulin as a new substrate of Esco1 in oocytes. We find that Esco1 is essential for normal spindle assembly and proper chromosome alignment by controlling α -tubulin acetylation-mediated microtubule stability to promote the meiotic progression in meiosis. Although we cannot rule out the possibility that Esco1 might contribute to the post-replicative cohesion establishment or non-cohesive activities of cohesin in oocyte meiosis because we indeed observed the chromosome localization of Esco1 during oocyte meiotic progression, our current observations assign a novel meiotic function to Esco1 as a microtubule regulator.

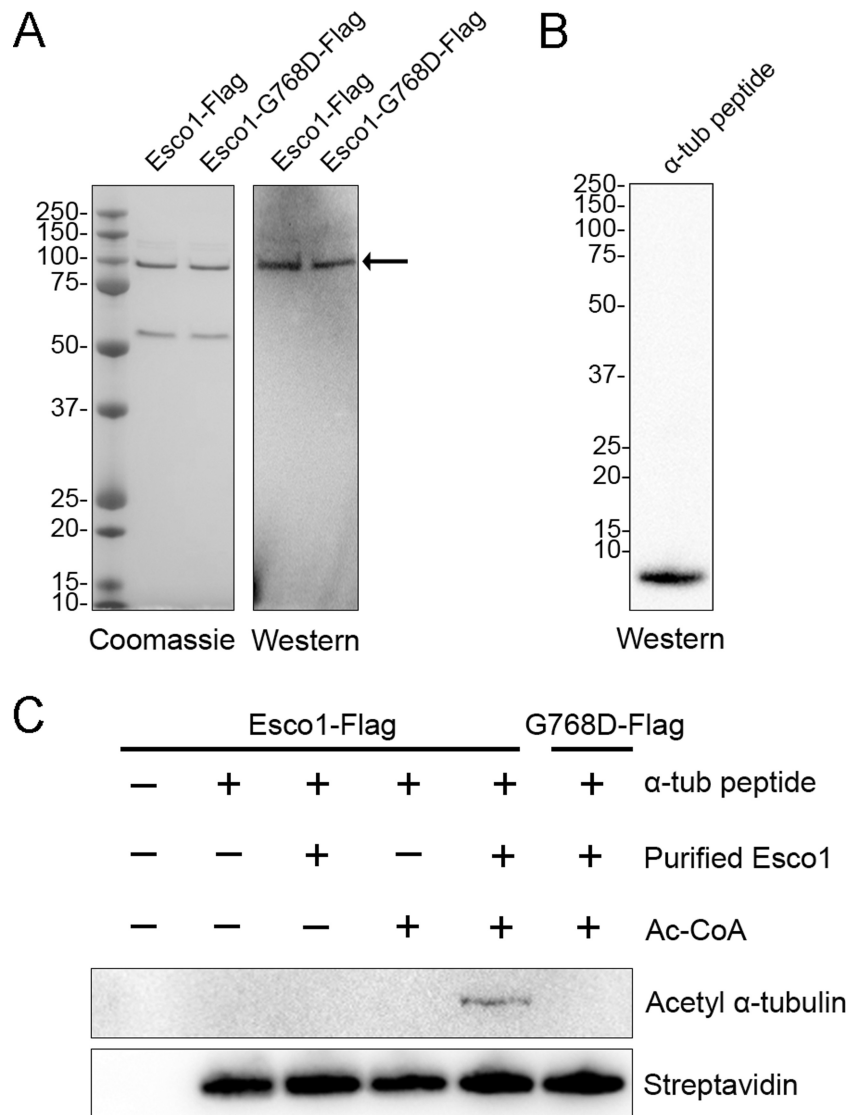


Figure 7. Purified Esco1 acetylates α -tubulin peptide *in vitro*. (A) Purification of Flag-tagged Esco1 proteins. Esco1 and enzymatically mutant Esco1-G768D were expressed in HEK293 cells and then purified according to the Flag purification procedure. Purified Esco1-Flag and Esco1-G768D-Flag were identified by coomassie staining and western blotting using anti-Esco1 antibody. (B) The synthesized peptide of α -tubulin was identified by western blotting using Streptavidin-HRP. (C) *In vitro* acetylation assay with purified Esco1 proteins and synthesized peptide. Synthesized α -tubulin peptide was incubated with or without purified Esco1-Flag, Esco1-G768D-Flag and Ac-CoA in the acetyltransferase assay buffer at 30°C for 1 h. The reactions were analyzed by western blotting with anti-acetyl- α -tubulin (Lys 40) antibody for acetylation levels of α -tubulin and Streptavidin-HRP as a loading control.

SUPPLEMENTARY DATA

Supplementary Data are available at NAR Online.

ACKNOWLEDGEMENTS

We would like to thank Dr Qiang Wang for providing antibodies.

Author contributions: Y.L. and B.X. designed the research; Y.L., S.L., Z.C., X.D., M.Z., Y.M. and C.Z. performed the experiments; Y.L., X.O. and B.X. analyzed the data; Y.L. and B.X. wrote the manuscript.

FUNDING

National Natural Science Foundation [31571545]; Natural Science Foundation of Jiangsu Province [BK20150677].

Funding for open access charge: National Natural Science Foundation [31571545].

Conflict of interest statement. None declared.

REFERENCES

1. Canela, N., Rodriguez-Vilarrupla, A., Estanyol, J.M., Diaz, C., Pujol, M.J., Agell, N. and Bachs, O. (2003) The SET protein regulates G2/M transition by modulating cyclin B-cyclin-dependent kinase 1 activity. *J. Biol. Chem.*, **278**, 1158–1164.
2. Qi, S.T., Wang, Z.B., Ouyang, Y.C., Zhang, Q.H., Hu, M.W., Huang, X., Ge, Z., Guo, L., Wang, Y.P., Hou, Y. *et al.* (2013) Overexpression of SETbeta, a protein localizing to centromeres, causes precocious separation of chromatids during the first meiosis of mouse oocytes. *J. Cell Sci.*, **126**, 1595–1603.
3. Nasmyth, K. and Haering, C.H. (2009) Cohesin: its roles and mechanisms. *Annu. Rev. Genet.*, **43**, 525–558.

4. Misulovin,Z., Schwartz,Y.B., Li,X.Y., Kahn,T.G., Gause,M., MacArthur,S., Fay,J.C., Eisen,M.B., Pirrotta,V., Biggin,M.D. *et al.* (2008) Association of cohesin and Nipped-B with transcriptionally active regions of the *Drosophila melanogaster* genome. *Chromosoma*, **117**, 89–102.
5. Parelho,V., Hadjur,S., Spivakov,M., Leleu,M., Sauer,S., Gregson,H.C., Jarmuz,A., Canzonetta,C., Webster,Z., Nesterova,T. *et al.* (2008) Cohesins functionally associate with CTCF on mammalian chromosome arms. *Cell*, **132**, 422–433.
6. Hakimi,M.A., Bochar,D.A., Schmiesing,J.A., Dong,Y., Barak,O.G., Speicher,D.W., Yokomori,K. and Shiekhattar,R. (2002) A chromatin remodelling complex that loads cohesin onto human chromosomes. *Nature*, **418**, 994–998.
7. Guacci,V., Koshland,D. and Strunnikov,A. (1997) A direct link between sister chromatid cohesion and chromosome condensation revealed through the analysis of MCD1 in *S. cerevisiae*. *Cell*, **91**, 47–57.
8. Uhlmann,F. (2004) The mechanism of sister chromatid cohesion. *Exp. Cell Res.*, **296**, 80–85.
9. Rowland,B.D., Roig,M.B., Nishino,T., Kurze,A., Uluocak,P., Mishra,A., Beckouet,F., Underwood,P., Metson,J., Imre,R. *et al.* (2009) Building sister chromatid cohesion: smc3 acetylation counteracts an antiestablishment activity. *Mol. Cell*, **33**, 763–774.
10. Unal,E., Heidinger-Pauli,J.M., Kim,W., Guacci,V., Onn,I., Gygi,S.P. and Koshland,D.E. (2008) A molecular determinant for the establishment of sister chromatid cohesion. *Science*, **321**, 566–569.
11. Rolef Ben-Shahar,T., Heeger,S., Lehane,C., East,P., Flynn,H., Shekel,M. and Uhlmann,F. (2008) Eco1-dependent cohesin acetylation during establishment of sister chromatid cohesion. *Science*, **321**, 563–566.
12. Hou,F. and Zou,H. (2005) Two human orthologues of Eco1/Ctf7 acetyltransferases are both required for proper sister-chromatid cohesion. *Mol. Biol. Cell*, **16**, 3908–3918.
13. Beckouet,F., Hu,B., Roig,M.B., Sutani,T., Komata,M., Uluocak,P., Katis,V.L., Shirahige,K. and Nasmyth,K. (2010) An Smc3 acetylation cycle is essential for establishment of sister chromatid cohesion. *Mol. Cell*, **39**, 689–699.
14. Ladurner,R., Bhaskara,V., Huis in 't Veld,P.J., Davidson,I.F., Kreidl,E., Petzold,G. and Peters,J.M. (2014) Cohesin's ATPase activity couples cohesin loading onto DNA with Smc3 acetylation. *Curr. Biol.*, **24**, 2228–2237.
15. Bolanos-Villegas,P. and Jauh,G.Y. (2015) Reduced activity of Arabidopsis chromosome-cohesion regulator gene CTF7/ECO1 alters cytosine methylation status and retrotransposon expression. *Plant Signal. Behav.*, **10**, e1013794.
16. Guacci,V., Stricklin,J., Bloom,M.S., Guo,X., Bhatner,M. and Koshland,D. (2015) A novel mechanism for the establishment of sister chromatid cohesion by the ECO1 acetyltransferase. *Mol. Biol. Cell*, **26**, 117–133.
17. Lu,S., Lee,K.K., Harris,B., Xiong,B., Bose,T., Saraf,A., Hattem,G., Florens,L., Seidel,C. and Gerton,J.L. (2014) The cohesin acetyltransferase Eco1 coordinates rDNA replication and transcription. *EMBO Rep.*, **15**, 609–617.
18. Bolanos-Villegas,P., Yang,X., Wang,H.J., Juan,C.T., Chuang,M.H., Makaroff,C.A. and Jauh,G.Y. (2013) Arabidopsis CHROMOSOME TRANSMISSION FIDELITY 7 (AtCTF7/ECO1) is required for DNA repair, mitosis and meiosis. *Plant J.*, **75**, 927–940.
19. Lu,S., Goering,M., Gard,S., Xiong,B., McNairn,A.J., Jaspersen,S.L. and Gerton,J.L. (2010) Eco1 is important for DNA damage repair in *S. cerevisiae*. *Cell Cycle*, **9**, 3315–3327.
20. Xiong,B. and Gerton,J.L. (2010) Regulators of the cohesin network. *Annu. Rev. Biochem.*, **79**, 131–153.
21. Lyons,N.A. and Morgan,D.O. (2011) Cdk1-dependent destruction of Eco1 prevents cohesion establishment after S phase. *Mol. Cell*, **42**, 378–389.
22. Guacci,V. and Koshland,D. (2012) Cohesin-independent segregation of sister chromatids in budding yeast. *Mol. Biol. Cell*, **23**, 729–739.
23. Strom,L. (2010) Additional proof for the importance of Eco1 for DNA double strand break repair. *Cell Cycle*, **9**, 3644.
24. Tanaka,K., Yonekawa,T., Kawasaki,Y., Kai,M., Furuya,K., Iwasaki,M., Murakami,H., Yanagida,M. and Okayama,H. (2000) Fission yeast Eso1p is required for establishing sister chromatid cohesion during S phase. *Mol. Cell Biol.*, **20**, 3459–3469.
25. Zhang,J., Shi,X., Li,Y., Kim,B.J., Jia,J., Huang,Z., Yang,T., Fu,X., Jung,S.Y., Wang,Y. *et al.* (2008) Acetylation of Smc3 by Eco1 is required for S phase sister chromatid cohesion in both human and yeast. *Mol. Cell*, **31**, 143–151.
26. Rahman,S., Jones,M.J. and Jallepalli,P.V. (2015) Cohesin recruits the Eco1 acetyltransferase genome wide to repress transcription and promote cohesion in somatic cells. *Proc. Natl. Acad. Sci. U.S.A.*, **112**, 11270–11275.
27. Alomer,R.M., da Silva,E.M.L., Chen,J., Piekarz,K.M., McDonald,K., Sansam,C.G., Sansam,C.L. and Rankin,S. (2017) Eco1 and Eco2 regulate distinct cohesin functions during cell cycle progression. *Proc. Natl. Acad. Sci. U.S.A.*, **114**, 9906–9911.
28. Zhang,S., Li,J., Zhou,G., Mu,D., Yan,J., Xing,J., Yao,Z., Sheng,H., Li,D., Lv,C. *et al.* (2016) Increased expression of ESCO1 is correlated with poor patient survival and its role in human bladder cancer. *Tumour Biol.*, **37**, 5165–5170.
29. Li,X., Liu,X., Gao,M., Han,L., Qiu,D., Wang,H., Xiong,B., Sun,S.C., Liu,H. and Gu,L. (2017) HDAC3 promotes meiotic apparatus assembly in mouse oocytes by modulating tubulin acetylation. *Development*, **144**, 3789–3797.
30. Skibbens,R.V., Corson,L.B., Koshland,D. and Hieter,P. (1999) Ctf7p is essential for sister chromatid cohesion and links mitotic chromosome structure to the DNA replication machinery. *Genes Dev.*, **13**, 307–319.
31. Toth,A., Ciosk,R., Uhlmann,F., Galova,M., Schleiffer,A. and Nasmyth,K. (1999) Yeast cohesin complex requires a conserved protein, Eco1p(Ctf7), to establish cohesion between sister chromatids during DNA replication. *Genes Dev.*, **13**, 320–333.
32. Burkhardt,S., Borsos,M., Szydłowska,A., Godwin,J., Williams,S.A., Cohen,P.E., Hirota,T., Saitou,M. and Tachibana-Konwalski,K. (2016) Chromosome cohesion established by Rec8-cohesin in fetal oocytes is maintained without detectable turnover in oocytes arrested for months in mice. *Curr. Biol.*, **26**, 678–685.
33. Tachibana-Konwalski,K., Godwin,J., van der Weyden,L., Champion,L., Kudo,N.R., Adams,D.J. and Nasmyth,K. (2010) Rec8-containing cohesin maintains bivalents without turnover during the growing phase of mouse oocytes. *Genes Dev.*, **24**, 2505–2516.
34. Portran,D., Schaedel,L., Xu,Z., Thery,M. and Nachury,M.V. (2017) Tubulin acetylation protects long-lived microtubules against mechanical ageing. *Nat. Cell Biol.*, **19**, 391–398.
35. Xu,Z., Schaedel,L., Portran,D., Aguilar,A., Gaillard,J., Marinkovich,M.P., Thery,M. and Nachury,M.V. (2017) Microtubules acquire resistance from mechanical breakage through intraluminal acetylation. *Science*, **356**, 328–332.
36. Robson,S.J. and Burgoyne,R.D. (1989) Differential localisation of tyrosinated, detyrosinated, and acetylated alpha-tubulins in neurites and growth cones of dorsal root ganglion neurons. *Cell Motil. Cytoskeleton*, **12**, 273–282.
37. Brown,R.C. and Lemmon,B.E. (2004) gamma-Tubulin, microtubule arrays, and quadrupolarity during sporogenesis in the hepatic *Aneura pinguis* (Metzgeriales). *J. Plant Res.*, **117**, 371–376.
38. Gadau,S.D. (2015) Detection, distribution and amount of posttranslational alpha-tubulin modifications in immortalized rat schwann cells. *Arch. Ital. Biol.*, **153**, 255–265.
39. Brown,R.C. and Lemmon,B.E. (2006) Polar organizers and girdling bands of microtubules are associated with gamma-tubulin and act in establishment of meiotic quadrupolarity in the hepatic *Aneura pinguis* (Bryophyta). *Protoplasts*, **227**, 77–85.
40. Ling,L., Hu,F., Ying,X., Ge,J. and Wang,Q. (2017) HDAC6 inhibition disrupts maturational progression and meiotic apparatus assembly in mouse oocytes. *Cell Cycle*, doi:10.1080/15384101.2017.1329067.
41. Lu,Y., Dai,X., Zhang,M., Miao,Y., Zhou,C., Cui,Z. and Xiong,B. (2017) Cohesin acetyltransferase Eco2 regulates SAC and kinetochore functions via maintaining H4K16 acetylation during mouse oocyte meiosis. *Nucleic Acids Res.*, **45**, 9388–9397.